Purdue University
Purdue e-Pubs

International Compressor Engineering Conference | School of Mechanical Engineering

2016

The Improvement of Motor Cooling Through Stator Profile Optimization using CFD Analysis in Hermetic Scroll Compressors

Weiping Tang
Danfoss (Tianjin) Ltd., China, People's Republic of, tangweiping@danfoss.com

Liu Wang
Danfoss (Tianjin) Ltd., China, People's Republic of, wangliu@danfoss.com

Li Yao
Danfoss (Tianjin) Ltd., China, People's Republic of, yaoli@danfoss.com

Jiangbo Lin
Danfoss (Tianjin) Ltd., China, People's Republic of, linjiangbo@danfoss.com

The Improvement of Motor Cooling Through Stator Profile Optimization Using CFD Analysis in Hermetic Scroll Compressors

Weiping TANG[1], Liu WANG[1], Li YAO[1*], Jiangbo LIN[1]

[1]Danfoss (Tianjin) Ltd., Danfoss Commercial Compressors
Tianjin, P.R. China
Phone: +86 22 82197029, Fax: +86 22 82197799, yaoli@danfoss.com

ABSTRACT

Hermetic compressor motor design face the challenge today that reducing the motor size for cost reason. This causes a higher motor power density and in turns a higher motor temperature. With the help of CFD computation tool, we investigated two ways to improve the motor cooling and bring the motor temperature down. One way is to put rotor ventilation channels to increase the flow in lower pressure side, so that the total percentage of suction gas to cool the motor increased. The other way is to optimize the stator cuts depending on flow rate in each stator cut. By combining these two improvement together, total motor temperature, particularly in stator end wing and rotor lower end ring, was reduced dramatically. Both motor and compressor prototype were tested and results given.

1. INTRODUCTION

With the increased pressure of cost, hermetic compressor sizing become an important part of the design optimization process, while maintain the same performance level in the same time. In order to squeeze the compressor to a minimum size and meanwhile maintain the same performance level, more thorough analysis and sophisticated methods and tools need to be utilized to achieve this goal.

This is also true for hermetic compressor motor design. A smaller motor size will still provide enough torque for the compression process, but with a relatively bigger current feeding to the motor. This leads to extra losses from the motor. From the overall compressor point of view, with this additional losses generated, in a given compressor load condition, when compressor reach thermal stability, motor temperature will become higher and might exceeds the limit required by regulation, or else the design already has some thermal margin to accommodate this increased temperature due to these added motor losses.

It has not been possible to visually check the temperature distribution as well as the gas flow inside the compressor shell, which is sealed against high pressure, so improvement of motor cooling has been a difficult problem for compressor motor designers. Compressor motor cooling improvement using thermal modelling has been investigated before by using thermal network method, Chen *et al.* (2012), with limited accuracy since this do not take all thermal correlation between motor and compressors. In recent years, Computational Fluid Dynamics (CFD) tools have been used to simulate refrigerant gas flow inside the compressor shell, as well as temperature distributions, and this helps designers to optimize the motor cooling.

2. ELECTRIC MOTOR LOSSES AND COOLING

The main losses inside a compressor including motor losses, compression losses, and also heat transfer losses. Here we concentrated on electric motor losses only. Motor losses include electromagnetic losses, and also mechanical losses, which are all dissipated by motor surroundings in the form of heat. The former losses can further be split into eddy current losses, hysteresis losses, copper losses and stray losses**.** Mechanical losses mainly from frictional losses between bearings and shafts.

Traditionally, core loss P_{Fe} can be divided into two components: hysteresis loss P_h and eddy current loss P_e. According to the Steinmetz equation, measurement and calculation of core losses are normally made with sinusoidal flux density of varying magnitude and frequency. These measurements and calculations are based on the standard coil and frequently modeled by a two term function of the form:

$$P_{Fe} = P_h + P_e = k_h f B^n + k_e f^2 B^2 \quad (1)$$

where f is the frequency of the external magnetic field, B is flux density, k_h , k_e and n are the coefficients, which depend on the lamination material, thickness, conductivity, as well as other factors. Stator copper losses are:

$$P_{Cu}= mI_1^2R_1 \quad (2)$$

Where m is the number of phases of the motor, I_1 is stator current, R_1 is stator resistance per phase. Rotor copper loss is:

$$P_{Al}= I_2^2R_2 \quad (3)$$

Where I_2 is rotor current, R_2 is rotor bar resistance include cage bars and end rings.

All these motor losses will turn into the format of heat, and to be dissipated by surrounding area, and reach a certain temperature when the system reaches thermal stability. Hermetic compressor motor is cooled by refrigerant inside the compressor, sometimes with oil also. Stator usually has cuts in the stator outer profile in order to let refrigerant pass through the gap between stator cores and compressor shell to cool the motor, and provide gas return path in the same time. Gas going into the suction port of the compressor is split into two parts, majority of the gas going into scroll set for compressor process, minor part of the gas will go through the stator cuts to low pressure side of the compressor, circulate through the stator lower winding and go back to motor top winding through stator cuts and air gap.

Factors that deciding motor temperatures are: how much motor losses generated and need to be dissipated and how effective this generated heat can be brought away, i.e. the cooling of the motor. Based on this, two major directions to reduce motor temperature can be inferred: (1) increase motor efficiency and reduce losses; (2) keep same motor efficiency level but improve the motor cooling.

Motor cost will be increased if we adding materials to the motor to improve motor efficiency, and this is not the preferred solution. However, it is more interesting to concentrated on optimizing the motor cooling path inside the compressor, such that motor temperature can be reduced but maintain the same cost.

3. COMPUTATIONAL FLUID DYNAMIC MODELE AND HEAT TRANSFER ANALYSIS

3.1 Computational Model

The computational model for inside the compressor of the lower pressure side is shown in Figure 1, where (a) is the compressor model and (b) is the entire mesh of the compressor model. Compressor is modelled from the oil surface to the housing thrust surface, because it is the most important part that related to motor cooling.

The computational model includes fluid domain and solid domain, the solid domain consist of stator, rotor, shaft, balancing counterweights, and suction baffle. The flow path of fluid domain is from the suction inlet of compressor to scroll suction port; while for motor flow path, which includes (1) the stator cut, and (2) the motor air gap which lie in between the circumference of the rotor and the inner circumference of the stator. The motor air gap (2) is very small, roughly 0.5mm per side, so constructing a mesh is difficult. However, since the motor air gap is very important in this motor cooling study, it is important that we include it in the computational model even though huge computation power needed.

The simulation method and calculation conditions are presented in Table 1. We selected FLUENT software to perform the computation, and there are several assumptions we have made also. The refrigerant gas is R410a, and it is considered as an incompressible fluid; oil channel cooling path in the middle of the shaft is neglected, since it is mainly to conduct the oil instead of the refrigeration gas and it is not directly cooling the stator and rotor; oil temperature is assumed to be constant for the computation and only steady state condition is considered, and no radiation heat transfer is considered. The fluid state equation we used in this study is k-ε equation with standard wall function.

Table 1: Simulation method and calculation condition

Computation method	Software	FLUENT
	Turbulent model	k-ε equation with standard wall function
	Mesh number	20,000,000 cells
Operating conditions	Rotation speed	3000 rpm
	Suction inlet pressure	11.5 bar
	Suction inlet temperature	299.7 K
	Discharge mass flow rate	0.1994 kg/s
	Oil temperature	366.5 K

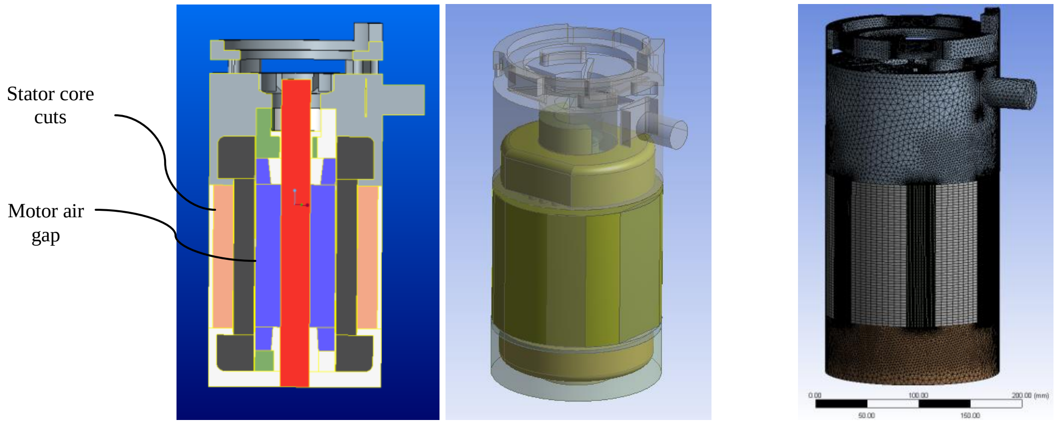

(a) Compressor model and motor cooling path (b) Entire mesh structure

Figure 1: Compressor model

3.2 Gas Flow Path and Heat Transfer Analysis

3.2.1 Refrigeration gas flow path distribution

Figure 2 shows the velocity distribution of the refrigerant gas flow for the standard stator cuts profile model. Figure 2 (a) shows the velocity vector distribution in one section, and (b) shows the gas flow direction. For the amount of suction gas into the compressor inlet, majority of the refrigeration gas goes into the scroll set, while a small portion goes down into stator cuts, particularly true in the stator cuts that adjacent to suction port, as can be seen in (b). These cooling gas then go down to the oil surface and return from the rotor air gap and also through the stator cuts that are opposite to the suction gas. Table 2 shows the percentage of each stator cuts flow in proportion to the total suction gas. Sign in Table 2 represent the direction of the flow; positive sign represent the downward direction, while negative sign represent the upwards flow direction.

Table 2: Percentage of flow in motor cooling path for motor with standard stator cuts

Section	Downward flow rate of cooling path, percentage to total suction gas	Section	Downward flow rate of cooling path, percentage to total suction gas
S1	4.04%	S4	-3.77%
S2	0.25%	S5	-0.16%
S3	-0.20%	S6	0.19%
S0	-0.35%	Total	4.48%

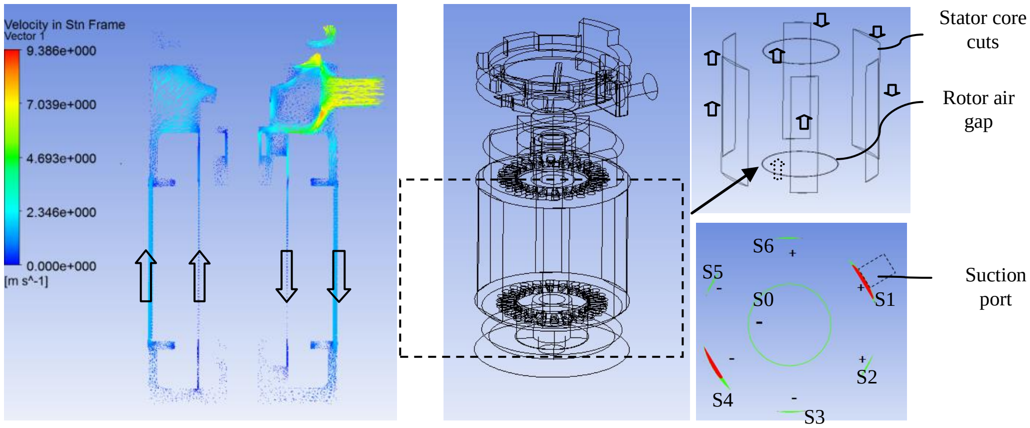

(a) Velocity vector distribution from one section view (b) Flow direction through the motor flow path

Figure 2: Velocity distribution for standard stator cuts

From the simulation result, we can see most of the refrigeration gas goes down to motor through stator cuts that next to suction port S1, and majority of them return through S4, which is the stator cuts that opposite to suction port. The total amount of refrigeration gas return through rotor air gap is small, due to the small air gap. The total amount of cooling gas goes down to cool the motor is 4.48% of the total suction gas, which is really small, and this is one aspects we want to improve.

3.2.2 Motor temperature distribution

Steady state heat transfer computation shows the temperature distribution inside compressor in low pressure side. Figure 3 (a) and (b) shows the temperature distribution cross sectional view, in different direction. Figure 3 (a) shows rotor temperature increases from top to bottom, due to the decreased cooling effects along the flow path. Bottom of rotor has the highest temperature. There is a sharp temperature distribution across the air gap because the existence of air gap and its heat transfer coefficient is much higher than solid. Figure 3 (b) shows the view cut in suction port direction, compare with (a), rotor temperature is with contoured distribution, temperature varies with the distance to suction port, if the distance is more close to the suction port, the temperature will be lower, valid in both axial and radial direction. And it is also the case for stator upper winding temperatures, as shown in Figure 3(c).

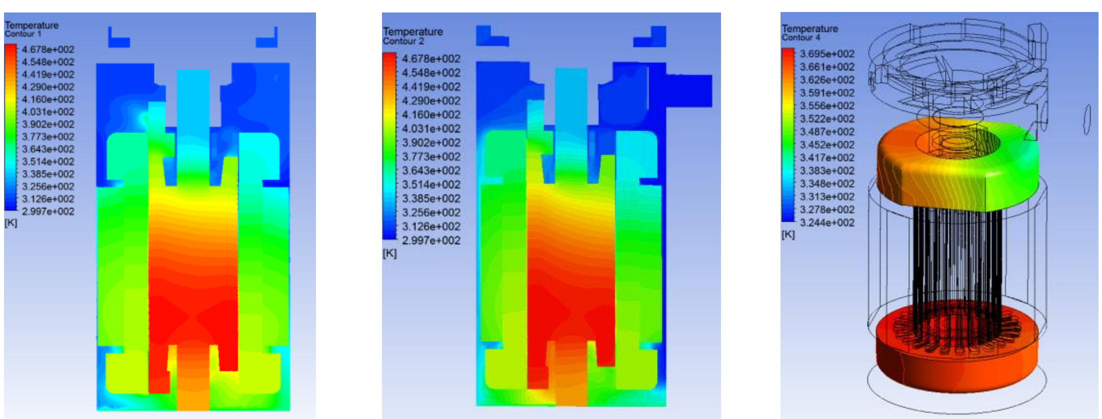

(a) Section view in orthogonal to suction (b) Section view of suction direction (c) stator windings temperature

Figure 3: Temperature distribution for compressor motor

Table 3 shows the temperature of each part of the compressor from CFD computation, in comparison with measurement results for stator upper-winding and stator lower-winding from test. Winding temperatures are measured by inserting thermocouples into the winding. Quite good alignment is found between simulation and test data. This model can be used to optimize motor cooling design. The main issue is that the bottom of motor temperature is too high; there will be insulation system lifetime risk. Further optimization need to be analyzed in order to reach this goal.

Table 3: Temperature for each part of the motor

Components	Temperature Computation (K) Delta to benchmark	Temperature Test (K) Delta to benchmark	Delta between test vs. calculation (K)
Stator upper-winding	benchmark	-15	-15
Stator lower-winding	+47	+39.7	-7.3
Rotor upper end-ring	+44	-	-
Rotor lower end-ring	+112	-	-

4. MOTOR COOLING OPTIMIZATION

The main target is to improve the motor cooling so reduce the motor temperature but maintain the similar motor performance in the same time. Two different cooling methods were investigated for the scroll type compressor motor, i.e. rotor cooling channels and optimized stator cuts profiles. Motor efficiency simulation results as well as CFD results for flow rate and also temperature distribution are given, prototype test also have been done to validate the methods.

4.1 Cooling Optimization on Rotor

Having additional cooling channels on rotor lamination is one of the popular choices for improved motor cooling, and this has been utilized for many other compressor motors, such as by Yokoyama *et al.* (2012). We also want to utilize this improvement for our study here.

4.1.1 Selection and optimization of ventilation channels on rotor
From simulation results in Table 2, only 4.48% of the total suction gas goes down to cool the motor, then flow back to scroll sets through air gap and opposite side of the stator cuts. For some compressor motor with a higher power density, this amount of cooling gas is not enough to bring the motor temperature down to accepted limit. To improve this situation, additional rotor channels are added to improve the cooling. However, the side effects of having channels on rotor lamination will squeeze the flux field (higher flux density) in rotor yoke area thus inducing higher magnetization current, leading to a lower motor efficiency.

Figure 4 shows the flux density impact of having rotor channels in flux distribution map. Flux distribution in rotor yoke increased due to the existence of these cooling channels. Care must be taken when selecting rotor channels not to have significant impact on motor efficiency.

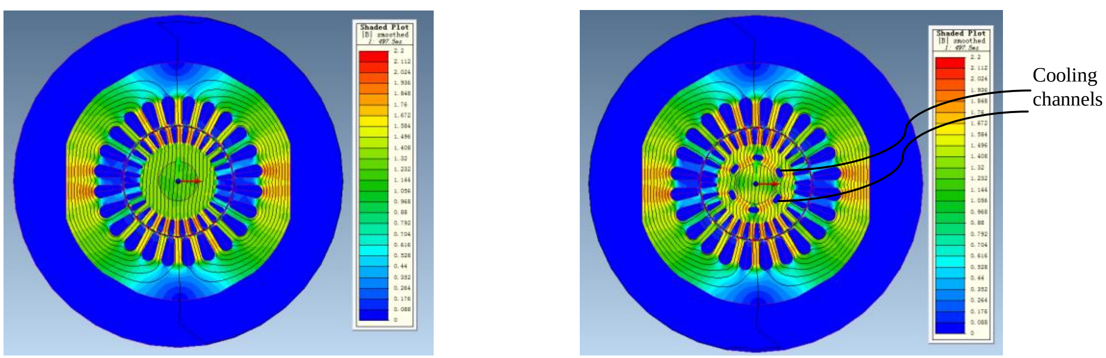

(a) Flux density distribution for a standard rotor (b) Flux density distribution of a rotor with channels

Figure 4: Motor flux distribution with cooling channels

Some important aspects need to be considered when design rotor channels, except the impact to motor efficiency. The motor design has a lower counterweight and end rings, these ventilation holes have to be placed between the inner diameter of the bottom of the end ring and the rotor shaft, to let the refrigeration gas pass through, as shown in Figure 5. From this point of view, there is not enough space to put reasonable sized round cooling holes, so kidney shaped holes are selected in this study. Important factors for selecting cooling holes include minimizing the windage losses and pressure loss but maintaining a maximum ventilation area and also the total circumferential length of the cooling channels, plus mechanical strength of the total rotor lamination with holes. Table 4 listed the key aspects. Figure 5 shows the dimensions of the kidney shape channels. Few optimization candidates are selected, and their area and position are shown in Table 5. We will select one of them to be our solution.

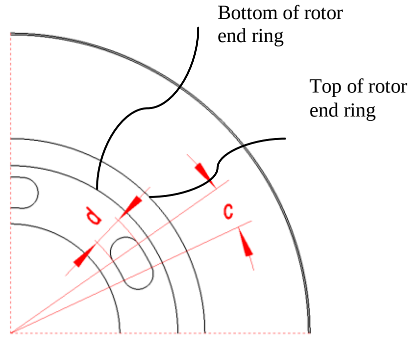

Figure 5: Rotor cooling channel dimensions

Table 4: Important factors to be considered when selecting rotor channels

	Comments
Winding loss	To be minimized
Total ventilation area	To be maximized
Total circumference length	To be maximized
Mechanical strength	Above certain level
Motor Efficiency	Least impact

Where: c: angle between the two center of the kidney shape cooling channel;
d: height of the kidney shape cooling channel in radial direction.

Table 5: Rotor cooling channel total area and circumference length

	Standard	**Design R1**	**Design R2**	**Design R3**
Comments	No holes on rotor	6 Holes on rotor, evenly distributed, 20 °separate	6 Holes on rotor, evenly distributed, 10 ° separate	4 Holes on rotor, evenly distributed, 20 °separate
c (degree)	0	20	10	20
d (mm)	0	4	4	4
Total ventilation area (mm^2)	0	229.1	152.3	152.8
Total circumference (mm)	0	152.3	113.8	101.5

4.1.2 Impact to motor efficiency of having ventilation holes
From the motor efficiency simulation results in Figure 6, we can see that with the increased number of cooling holes on rotor, motor efficiency reduced as expected, due to the increased losses. With the same ventilation area, the more the number of holes, the more efficiency reduction. Design R2's motor efficiency is the highest among the three designs, and its total circumference is larger than design R3, while the total ventilation area is the same as design R3. So it is the best option that we will go forward with prototypes and testing.

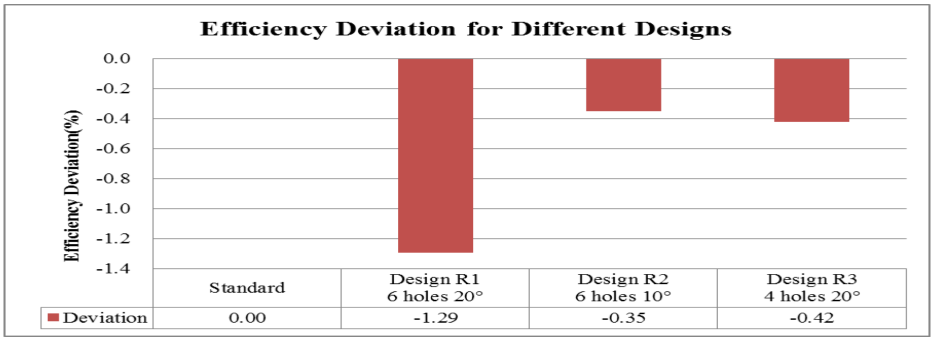

Figure 6: Efficiency comparison for different designs, motor simulation results

A prototype rotor was made with deign R2, 6 holes 10 °separate. Motor efficiency is measured with dynamometer. Measurement results in comparison with original motor efficiency benchmark ηs without ventilation holes are shown in Table 6. These tests are performed in rated (ARI) condition torque.

Table 6: Test results comparison between original motor vs. design R2 rotor

	Efficiency [%]				**Current [A]**			
	Test	Deviation (absolute value)	Calculation	Deviation (absolute value)	Test	Deviation (absolute value)	Calculation	Deviation (absolute value)
Standard	101.72% *ηs	--	ηs	--	97.71% * *Is*	--	*Is*	--
Design R2 6 holes 10 ° separate	101.26% *ηs	-0.41%	99.60% *ηs	-0.35%	99.88% * *Is*	0.36A	103.13% * *Is*	0.52A

Motor current increased by 0.36A, and total motor efficiency reduced by 0.41%. From simulation results, motor current increase by 0.52A, and total motor efficiency reduced by 0.35%. They are close enough for us to trust the motor simulations.

4.1.3 CFD simulation results – with ventilation channels on rotor

Table 7 shows the change of flow rate in each part of the cooling path, in terms of percentage to total suction inlet refrigerant gas. The total amount of gas that flow directly down to motor increased from 4.48% to 6.43%, and particularly, the amount of gas flow through S1, which is the stator cuts besides the suction port; S2 and S6, which are the stator cuts close to suction port, have been increased by 1.25%, 0.11%, 0.11% respectively. These flow rates are increased by having these ventilation holes on rotor. Figure 7 shows the position for rotor ventilation holes, i.e. Sl1 to Sl6. In Table 7, positive sign represent downward flow, while negative sign represent upward flow.

Table 7: CFD results for flow rate between standard designs vs. design R2 in percentage of total suction gas

Section	Downward flow rate of cooling path		Deviation
	Standard	Design R2	
S1	4.04%	5.29%	1.25%
S2	0.25%	0.36%	0.11%
S3	-0.20%	0.09%	0.29%
S4	-3.77%	-2.89%	0.88%
S5	-0.16%	0.07%	0.23%
S6	0.19%	0.30%	0.11%
S0	-0.35%	0.32%	0.67%
Sl1	--	-0.57%	-0.57%
Sl2	--	-0.58%	-0.58%
Sl3	--	-0.58%	-0.58%
Sl4	--	-0.59%	-0.59%
Sl5	--	-0.60%	-0.60%
Sl6	--	-0.61%	-0.61%
Total	4.48%	6.43%	1.95%

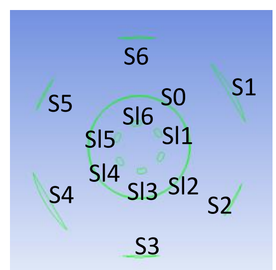

Figure 7: Ventilation holes position

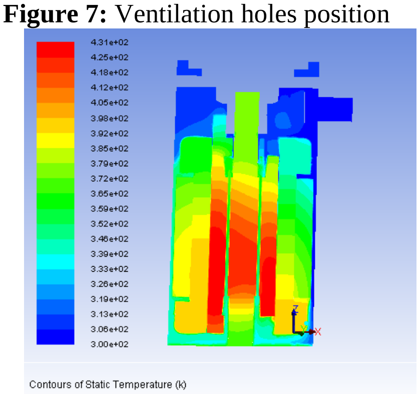

Figure 8: Temperature distribution with ventilation holes

Figure 8 and Table 8 shows the temperature distribution for the motor and also the temperature for each part. We can see that having holes on rotor has a bigger impact on bottom winding of the stator, and even better effects for rotor temperature by itself. This cooling method is preferred if we want to reduce rotor temperature particularly. For our research in this paper, the reduction of stator end winding temperature is still not enough, so further optimization need to be invested as well.

Table 8: CFD simulation result of design R2 in comparison with original design

Component	Temperature reduction from Computation (K) Compare to standard design
Stator upper-winding	-4
Stator lower-winding	-7
Rotor upper end-ring	-14
Rotor lower end-ring	-42

4.1 Cooling Optimization for Complete Motor

With additional ventilation channels on rotor, flow rate on stator cuts also changes, and S1, S2 and S6 flow rate have been increase as the results; but S3, S4 and S5 flow rate reduced, due to the existence of rotor holes. To better accommodate the increased flow down to motor from suction side, we decided to increase the stator cuts in S1, S2, and S6, to allow more gas going through, and keep same stator cuts on S3, S4 and S5, since their flow rate reduced with ventilation holes.

On the other hand, more stator cuts will reduce the yoke thickness of the stator, introducing higher flux density in that area, so to cause higher magnetization current thus more iron losses, especially we already have holes on rotor for ventilation. In order to find the optimized stator cuts, we made several options. Figure 9 shows the dimension of the stator cuts. Cuts parameter *a* vary from 0.5mm to 3mm, 0.5mm per step; parameter *b* vary from 0.5mm to 2mm, 0.5 mm per step. There are 24 combinations in total. Each individual option is evaluated with motor efficiency simulation first.

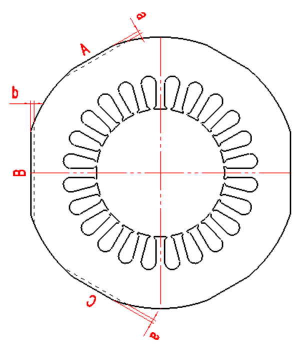

Figure 9: Stator cuts dimensions

In order to select the optimal stator cuts, another important factor we need to consider is the total shrink fit area of the stator with respect to the compressor shell. A certain shrink fit area between stator outer diameter and compressor shell has to be maintained to ensure the stator will not turn inside the shell during operation and transients. Figure 10 show the shrink fit circumference, total ventilation area, and also motor efficiency for different combinations. Motor efficiencies are calculated without ventilations holes on rotor.

For the total ventilation area, we can see that change of parameter *a* has more impact on ventilation area than parameter *b*, and has less adverse impact to motor efficiency as well. Depending on what aspects we want to optimize our design, we can select different combination which suits the design purpose the best. From Figure 10, design *a*=2.5, *b*=1, and *a*=3, *b*=0.5, combinations are selected; they both have the relatively big ventilation area without too much impact to motor efficiency. Next, *a*=2.5 and *b*=1 is selected for final investigation.

In previous text, two different cooling improvement methods have been proposed and validated; on rotor and stator respectively, now we want to combine these two together, to further investigate what is the benefit in terms of motor cooling and the impact to motor efficiency as a whole.

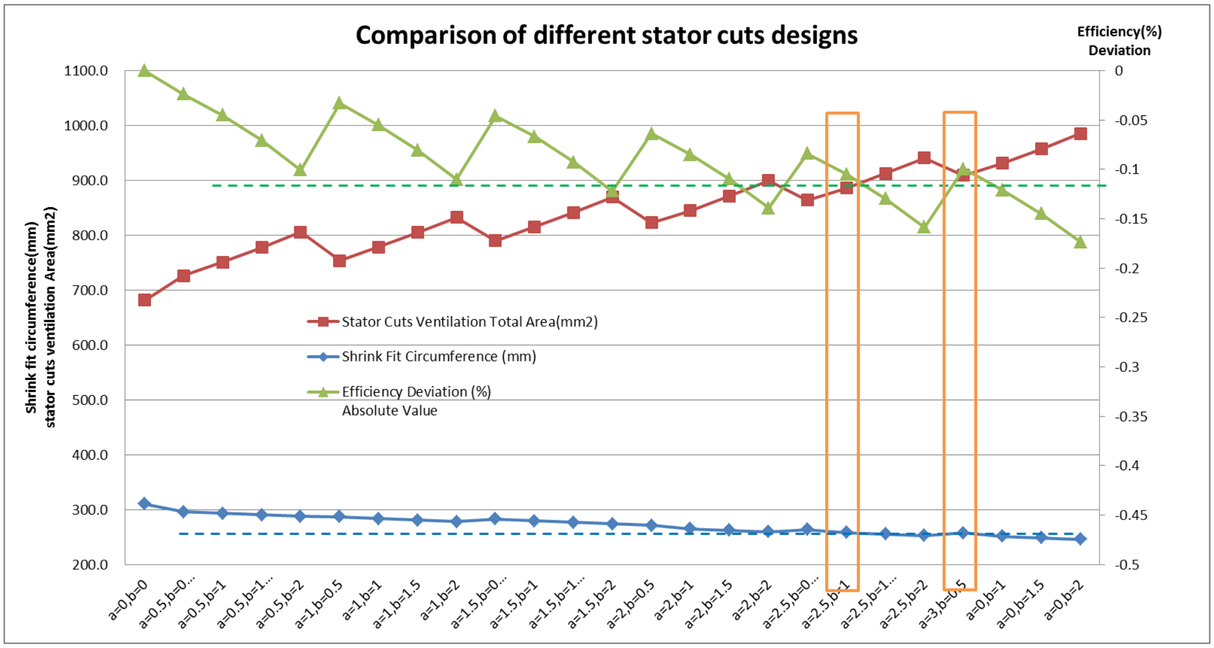

Figure 10: Comparison for different stator cuts designs

4.2.1 Impact to motor efficiency – combination of optimization on stator and rotor
Table 9 shows the simulation and prototype results for design R2, 6 rotor ventilation holes with 10° separate, combined together with stator cuts *a*=2.5, *b*=1 design, taking the calculated value for standard design as the benchmark. Motor efficiency dropped by 0.46% from calculation, this aligns with rotor ventilation holes efficiency impact (-0.35%, Table 6) plus stator cuts efficiency impact (-0.1%, Figure 10). Test results are well accepted within this cooling improvement.

Table 9: Motor test and simulation results with stator cuts and rotor cooling holes @ rated condition compare to standard design

	Efficiency [%]				Current [A]			
	Test	Deviation (absolute value)	Calculation	Deviation (absolute value)	Test	Deviation (absolute value)	Calculation	Deviation (absolute value)
Standard	101.7%* *ηs*	--	*ηs*	--	97.7%* *Is*	--	*Is*	--
Design R2 6 holes 10° with stator cuts *a*=2.5, *b*=1	101.3%* *ηs*	-0.37%	99.5%* *ηs*	-0.46%	100.7%* *Is*	0.49A	104.1%* *Is*	0.68A

4.2.2 CFD results for optimized combined cooling design
Table 10 shows the CFD computation results for temperatures. We can conclude that:

- The temperature of stator upper-winding decreased about 7 K, this will do benefit for the motor protection selection and matching.
- The temperature of stator lower-winding decreased 22 K, this is really a huge benefit for complete motor temperature, so to insulation life etc.
- For rotor temperature, which is the most difficult part to cool, the optimization seems to be very effective, temperature decreased from 21 K to 60 K, depending on position.

Table 10: Simulated temperature for each part for standard design in comparison to optimized design

Component	Temperature reduction from Computation (K) Compare to standard design
Stator upper-winding	-7
Stator lower- winding	-22
Rotor upper end-ring	-21
Rotor lower end-ring	-60

4.2.3 Compressor test results for the optimized cooling design
Compressor sample was tested with thermocouples inserted into the stator windings. Table 11 shows the comparison results for the optimized design with standard design. Stator upper winding temperature decreased by 17.4 degree; and lower winding temperature decreased by 26.2 degree. This is very promising temperature improvement and can be utilized in future design.

Table 11: Compressor temperature measurement results between final optimized design and standard design

Component	Deviation (K) Test results Optimization vs. standard
Stator upper-wingding	-17.4
Stator lower-winding	-26.2

5. CONCLUSIONS

We investigated how to improve hermetic scroll compressor motor cooling by performing CFD analysis. Flow and temperature analysis were done to help with the investigation. Two methods to improve the motor cooling:

(1) By carefully selecting rotor ventilation channels, considering different factors, total percentage of gas going into low pressure side increased. Stator lower winding temperature reduced by 7 degree from CFD simulation. Rotor lower end ring temperature reduced by 42 degree.
(2) Optimize stator cuts to accommodate flow rate in different cuts position, on top of the rotor ventilation channels optimization, which proved to be very effective. Stator lower winding temperature reduced by 22 degree from simulation, and 26.2 degree from test. Rotor lower end ring temperature reduced by 60 degree from simulation.

Compressor test results confirmed the effectiveness of the combined optimization of motor cooling. Stator upper winding and lower winding temperature were reduced by 17.4 degree and 26.2 degree respectively, which is very promising and exciting way to improve motor cooling for motor and compressor designers.

REFERENCES

Chen, W., Shen J., He J., Wu H., Xing Z., (2012). Thermal Modelling for the Motor in Semi-hermetic Screw Refrigeration Compressor under Part-load Conditions. *Proc. Int. Compressor Engineering Conference at Purdue, C1246.*

Yokoyama, T., Shingu K., Sekiya S., Maeyama H., Nishimura N., (2012). CFD Analysis inside a CO2 Rotary Compressor Shell to Improve Oil Separation and Reduce the Shell Size. *Proc. Int. Compressor Engineering Conference at Purdue, C1230*.